ALS BEAMLINE 6.0 FOR ULTRAFAST X-RAY ABSORPTION SPECTROSCOPY

P.A. Heimann[a*], H.A. Padmore[a], and R.W. Schoenlein[b]

[a]*Advanced Light Source, Lawrence Berkeley National Laboratory, Berkeley, CA 94720, USA*
[b]*Materials Sciences Division, Lawrence Berkeley National Laboratory, Berkeley, CA 94720, USA*

Abstract. Beamline 6.0 is designed for x-ray absorption spectroscopy with femtosecond x-ray pulses generated by the 'slicing' technique. The fs x-ray pulses are isolated by imaging the source and translating slits a small vertical distance from the optical axis. Soft and hard x-ray branch lines will cover a wide photon energy range from 120 eV to 10 keV. A soft x-ray spectrograph will collect absorption spectra dispersively.

INTRODUCTION

An insertion device beamline 6.0 will be dedicated for time-resolved x-ray science. It is specifically designed to provide high flux over a photon energy range including both soft and hard x-rays. The beamline incorporates optical components specifically chosen to accommodate femtosecond x-ray pulses by providing low non-specular scattering. A high-average-power, femtosecond laser system will be located at the end of the beamline. The location of beamline 6.0 at the straight section immediately following the wiggler 5.0 minimizes the electron time-of-flight contribution to the x-ray pulse duration. Based on the known storage ring parameters and our characterization measurements, we expect that x-ray pulses of 200 fs can be generated from this beamline.

Since the time-resolved x-ray experiments will generally operate at a fraction of the synchrotron bunch repetition frequency (500 MHz), high efficiency in the beamline design is required in order to deliver the maximum possible number of x-ray photons onto the sample. The laser system will operate at a repetition rate of 40 kHz. In the soft x-ray range, dispersive methods are employed. Pink beam is imaged onto the sample and subsequently dispersed in a grating spectrometer, thus making use of the full bandwidth of an undulator harmonic.

Another important consideration in the beamline design is the isolation of the femtosecond x-ray pulse from the long-pulse x-ray background originating from unperturbed electrons. The laser pulse modulation of the electron beam energy combined with a vertical dispersion bump in the storage-ring lattice, will cause a fraction of the particles ($\sim 10^{-3}$ of the electrons in a bunch) to be vertically displaced within the wiggler / undulator by a distance of Δy. For $D_y = 4$ cm and a maximum energy modulation of 17 MeV, an optimal displacement for the sliced pulse is $\Delta y = 280$ μm. A pair of slits at an image plane of the wiggler / undulator source (displaced Δy above the optic axis) will then select the femtosecond x-ray pulses and block the long-pulse background.

Previous measurements were performed of the profile of the electron beam in the ALS.[1] The electron beam lifetime was measured as a function of the horizontal scrapper position. From this experiment it was determined that the transition from the Gaussian beam core to the more slowly decreasing tails occurs at the 6σ point, a background level of 2×10^{-8}.

Creating a clean image of the source is critical for minimizing the background. Non-specular scattering in the vertical plane will be minimized by using a single, sagittally focusing mirror. Qualitatively, the advantage of a sagittally focusing mirror can be understood from by considering the different length scales of roughness contribute to in-plane and out-of-plane scattering.[2] These relevant length scales are given by the off-plane grating equation:

$$m\lambda = d\,[(1 + z^2/r^2)^{-1/2} \sin\alpha + (1 + z'^2/r'^2)^{-1/2} \sin\beta]$$

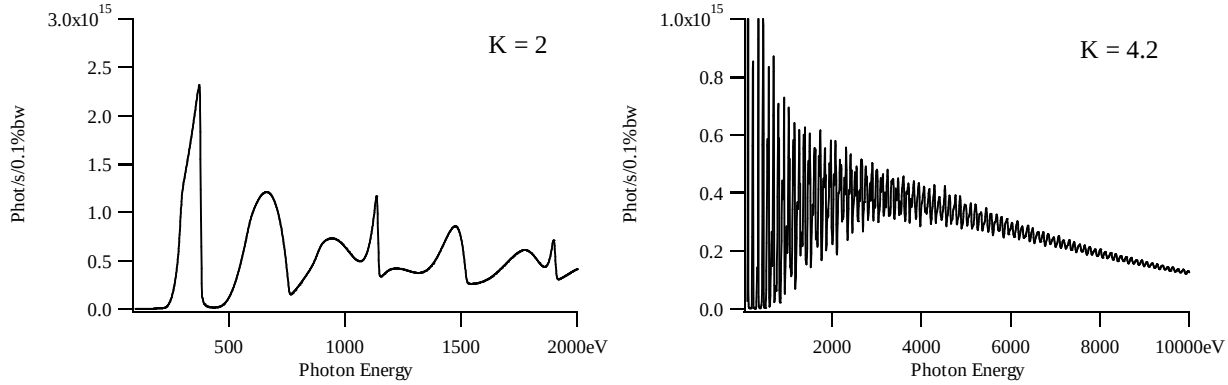

FIGURE 1. Undulator spectrum calculated with SRW. Calculated for 3 cm period.

where m is the diffracted order, λ the wavelength, d the spatial period of the roughness, z and z' the source and image distances out of the plane defined by the mirror normal and by the line along which the mirror roughness is measured, r and r' the source and images distances projected in that plane and α and β the incident and diffracted angles. At 5000 eV photon energy the first mirror M21 has a relevant spatial period for scattering of 1 mm in the tangential geometry and 10 μm in the sagittal geometry. In general, the amplitude of optical roughness decreases dramatically with the spatial period. Consequently, there is an advantage to using the sagittal focusing geometry.

The source is an in-vacuum permanent magnet insertion device. It has 50 periods with a λ_u of 30 mm and a peak magnetic field of 1.5 T. At low photon energies, below 2 keV undulator harmonics are accepted in a relatively large angular aperture of 0.5 mrad horizontal x 0.5 mrad vertical. Extending the angular aperture beyond the central cone increases the width of the odd harmonics and increases the intensity of the even harmonics. At high photon energies, above 2 keV the source is wiggler radiation in a 0.5 mrad horizontal x 0.3 mrad vertical aperture. The insertion device spectrum calculated by the program SRW is shown in figure 2.[3] Magnetic field errors are not included in the calculation. Two K values are shown: 2 and the maximum value of 4.2. The broad, even harmonics are attractive for EXAFS measurements. Above 2 keV, the spectrum is a modulated continuum of the wiggler radiation. By using both undulator and wiggler radiation a wide photon energy range is provided from 120 eV to 10 keV.

FIRST MIRRORS, CHOPPERS AND SLITS

The first optical element of both soft and hard x-ray branch lines is a toroidal mirror, which produces an image of the insertion device source. The grazing incidence angles of 1.35 degrees and 8 mrad result in energy cut-offs of 2000 eV and 10 keV for the soft x-ray M11 and hard x-ray M21 mirrors respectively. The side-cooled mirrors are polished as cylinders and bent into toroids. The M21 mirror provides an image of the source[4] at 1:1 magnification, 720 μm horizontal by 100 μm vertical. The M11 mirror has a somewhat reduced magnification, 0.79.

The effect of the wiggler source length on the background has been analyzed by ray tracing and an analytical model. The wiggler has a 1.5 m length and radiation is accepted over a 0.3 mrad vertical aperture. The analytical model includes an integration over the length of the source contributing at the given position and a convolution with the Gaussian electron beam. The aberrations of the toroidal mirror are included in the raytracing. The background at 290 μm from the optical axis reaches a level below 10^{-5}. These results suggest that the contributions of source length and mirror aberrations to the background are acceptable.

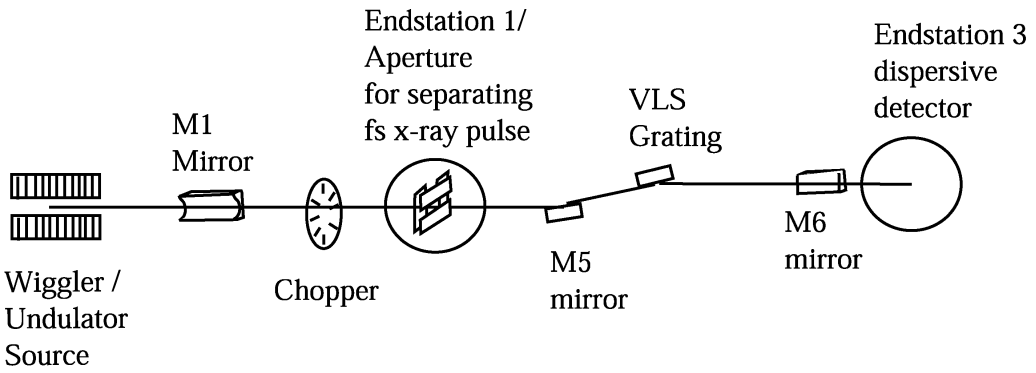

FIGURE 2. Schematic layout of the soft x-ray branch line**.**

Following the M11 and M21 mirrors are an x-ray chopper, which act as a power filter and has a repetition rate matched to the laser system. The chopper is located near the waist of the intermediate focus produced by the M1 mirror. The chopper openings (slits) can be matched to the x-ray beam size (4σ) at this location, 300 μm for the soft x-ray branch and 200 μm for the hard x-ray branch. The power absorbed in the chopper is 130 W for the soft x-ray branch and 430 W for the hard x-ray branch. The design of the chopper is based on a rotating anode. The disk, rotating in vacuum, is mounted on a water-cooled tube, which passes through a ferrifluidic seal. The heat load on the optics after the chopper is much reduced, 4 W for the soft x-ray branch and 9 W for the hard x-ray branch. Following the choppers, horizontal / vertical pairs of slits are used to select the femtosecond x-ray pulses.

GRATING SPECTROGRAPH

Table 1 lists the optical elements of the varied line spacing (VLS) grating spectrograph / monochromator. VLS grating spectrographs provide flat-field imaging at the detector, i.e. a whole spectrum is in focus in a plane perpendicular to the optical axis.[5] The total number of reflections including the M1 mirror is four. Three different M5 mirrors alternatively produce a converging beam for the VLS grating at deviations angles. The different M5 mirror deviation angles provide optimal efficiency over different grating photon energy rangesThe 150 mm^{-1} grating provides a wider energy window while the 600 mm^{-1} grating delivers higher resolution. Both gratings operate in positive order. . The M5 mirrors and gratings are side cooled. The M6 mirror provides a horizontally demagnified (13 times) image of the intermediate focus onto the detector. In spectrograph mode the sample is located following the aperture for separating the fs x-ray pulses and a multi-channel detector is located at the end of the spectrograph.

The goal of energy resolution is 0.5 eV at 850 eV photon energy determined by the natural linewidth of the nickel L_3 edge. This goal is achieved. The energy resolution is 0.56 eV at 850 eV with a 70 μm entrance slit. The slit width is chosen to match the vertical image of the central cone radiation. The magnification of the M12 mirror is set to one while the average magnification of the grating is about 0.5.

TABLE 1. Optical elements of the soft x-ray branch line.

	Type	Coating , Blank	Dimensions (mm)	Radius (m)	Incidence angle (°)	Grating d (mm^{-1}), m
M11	Toroidal mirror	Pt-coated silicon	320 x 90 x 25	449 (R) 0.2472 (ρ)	88.655	-
M12	Spherical mirror	Ni, Pt-coated silicon	60x70x25 80x70x25 100x70x25	63 90 126	87 87.9 88.5	-
G1,G2	VLS, Plane grating	Ni, Pt-coated silicon	167x36x30	∞	84 – 90	1/150, +1 1/600, +1
M13	Plane elliptical mirror	Pt-coated fused silica	220 x 40 x 25	33.4	88.5	-

The energy window across the detector is limited at low photon energies. At the C edge 280 eV the window is 64 eV. This spectral range is sufficient for XANES measurements but not for EXAFS. There is a compromise between having an instrument optimized for high spectral resolution vs. wide spectral range. The VLS grating coefficients may be the same for different deviation angles. The aberrations of the M5 mirror are small because of the magnification of one.

We take as the standard detector for the spectrometer a streak camera with a grazing incidence photocathode. Having the x-rays hit the photocathode at grazing angle proides near unity quantum efficiency. The electrons are imaged by a magnetic lens onto a CCD camera. For the spectrometer design a spatial resolution of 25 μm is assumed, which has been achieved by the streak camera in unswept imaging tests.

The grating diffraction efficiencies for laminar profiles are calculated from the Neviere theory of grating efficiency.[6] The grating efficiencies are optimized for different groove depths, groove widths and coatings. A photon energy range of 125 – 1800 eV is covered. The groove width is optimized as well. The total efficiency of the soft x-ray branch line is, for example, 17 % at 280 eV.

The soft x-ray spectrograph should be designed to collect off-axis undulator radiation to provide sufficient bandwidth for x-ray absorption spectroscopy. The angular acceptance 0.5 (h) x 0.5 (v) provides a sufficient width of the undulator harmonics to fill the photon energy window of the spectrometer's detector.

The fs x-ray pulse can be stretched by grating optics. In the case of the grating spectrograph there is no time stretching because the grating is after the sample. In monochromator mode, the time stretching can be estimated from N λ, where N is the number of illuminated grooves. For the example of 280 eV the pulse stretching is only 30 fs, because the angular aperture can be limited to the undulator central cone radiation.

CRYSTAL MONOCHROMATOR

The design of the crystal monochromator branch line is similar to ALS micro x-ray absorption spectroscopy beamline 10.3.2. The M2 mirror collimates the x-ray beam into the crystal monochromator. For the crystals the collimation reduces the beam divergence contribution to the energy resolution. Si(111) or Ge(111) crystals are used to monochromatize the x-rays. Ge(111) crystals have higher integrated reflectivity while Si(111) crystals have higher energy resolution. Finite element analysis showed Ge(111) crystals to have unacceptable thermal distortion with the full x-ray power of 7 W. As a result, the Ge(111) crystals will only be used with the fs x-ray pulses at much reduced power. The photon energy range is 2.28 - 10 keV. The M4 and M5 mirrors refocus the x-rays focus into the second endstation. In the Kirkpatrick and Baez geometry, the M4 mirror produces a vertical focus at 1 to 1 magnification while the M5 mirror demagnifies the beam horizontally by 6 to 1. For the M4 and M5 mirrors, raytracing shows a focus of 110 μm horizontal x 100 μm vertical in the endstation.

The efficiency of the hard x-ray branch line has been calculated. The crystal efficiencies are evaluated from the integated reflectivity, $R^2(\theta)$, calculated with the program XOP.[7] At 7 keV the branch line efficiency normalized to 0.1% bandwidth is 10 % for the Ge(111) crystals and 4.5 % for the Si(111) crystals. In the future the possibility of using dispersive optics for hard x-ray energies should be evaluated.

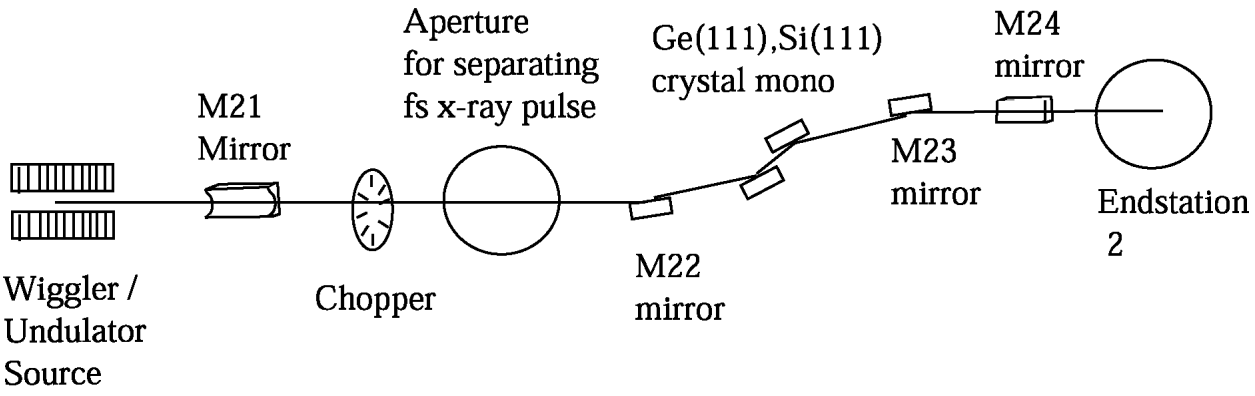

FIGURE 3. Schematic diagram of the crystal monochromator branch line.

TABLE 2. Optical elements of the hard x-ray branch line 6.0.

	Type	Coating , Blank	Dimensions (mm)	Radius (m)	Incidence angle (°)
M21	Toroidal mirror	Pt-coated silicon	800 x 40 x 75	1458 (R) 0.0933 (ρ)	89.54
M22	Cylindrical mirror	Pt-coated silicon	150 x 12 x 6	750	89.54
X1, X2	Crystal	Si (111), Ge(111)	20 x 10 x 10	∞	6 - 60 (θ_B)
M23	Cylindrical mirror	Pt-coated silicon	150 x 12 x 6	750	89.54
M24	Plane elliptical mirror	Pt-coated fused silica	600 x 40 x 50	160	89.54

ACKNOWLEDGMENTS

We would like to acknowlege the efforts of the ALS engineers: Nord Andresen, Barry Bailey, Daniela Cambie, Curtis Cummings, Robert Duarte, Michael Fahmie, Alan Paterson, David Plate and Troy Stevens

REFERENCES

1. Zholents, A., and Decking, W., LBNL Report No. 45392, 1999.
2. Church, E.L, and Takacs, P.Z., Opt. Eng. 34, 353-360 (1995).
3. Chubar, O., Elleaume, P., Proceedings of the EPAC98 Conference, 1177-1179 (1998).
4. http://www-als.lbl.gov/als/SRparameters.html
5. Underwood, J.H., and. Koch, J.A, Applied Optics 36, 4913-4921 (1997).
6. Electromagnetic Theory of Gratings, edited by R. Petit, Springer-Verlag, Berlin, 1980.
7. Sánchez del Río, M., and Dejus, R. J., SPIE Proceedings 3152, 148-157 (1997).